Ab Initio Computational Studies of Conformationally Restricted Cope Rearrangements. First Examples of Fully Concerted Allenyl Cope Rearrangements

James A. Duncan* and Marie C. Spong†

Department of Chemistry, Lewis & Clark College, Portland, Oregon 97219-7899

duncan@lclark.edu

Received April 17, 2000

Results of (8,8)CASPT2/6-31G*//(8,8)CASSCF/6-31G* level calculations on the potential surface for the conformationally restricted allenyl Cope rearrangements of *syn*-5-propadienylbicylco[2.1.0]-pent-2-ene (**14**) and *syn*-6-propadienylbicyclo[2.1.1]hex-2-ene (**15**) are reported. Both are found to proceed through concerted pathways. Also included are the results of (6,6)CASPT2/6-31G*//(6,6)-CASSCF/6-31G* level calculations on the Cope rearrangements of *syn*-5-ethenylbicyclo[2.1.0]pent-2-ene (**18**), *syn*-6-ethenylbicyclo[2.1.1]hex-2-ene (**19**), and *syn*-7-vinylnorborene (**20**), which are found to involve diallylic diradical intermediates **26**, **30**, and **36**, respectively. Previous studies have shown that the allenyl Cope rearrangement of 1,2,6-heptatriene (**1**) to 3-methylene-1,5-hexadiene (**2**) involves a single transition structure that either proceeds to the monoallylic cyclohexane-1,4-diyl derivative **3** or bypasses **3** to form **2** directly.[4] More recently, the conformationally restricted allenyl Cope rearrangement of *syn*-7-allenylnorbornene (**7**) has also been found to involve tricyclic monoallylic cyclohexane-1,4-diyl intermediate **11**.[7] The rearrangements of **14** and **15** appear to represent the first reported examples of fully concerted allenyl Cope rearrangements. Concertedness in these cases is ascribed to two parallel factors: (1) the relative instability of possible tricyclic diradical intermediates **16** and **17**, compared to diradical intermediates **3** and **11** formed in the rearrangements of **1** and **7**, respectively; and (2) the opportunity that exists to form sp-sp^2 σ bonds in transition structures **21** and **23** that lead, respectively, to products **22** and **24**. By contrast, only weaker sp^2-sp^2 σ bonds could form in unobserved concerted transition structures leading to products **28** and **32**, formed in the nonconcerted rearrangements of **18** and **19**.

The Cope rearrangement has been the subject of numerous experimental and theoretical studies.[1] In particular, (6,6)CASSCF/6-31G* level calculations on the paradigmatic Cope rearrangement of 1,5-hexadiene, that included dynamic electron correlation using either CASPT2[2] or CASMP2[3] versions of multireference perturbation theory, have shown that it proceeds only by way of a concerted reaction.[1g,1h]

On the other hand, calculations and experimental investigations on the parent *allenyl* Cope rearrangement of 1,2,6-heptatriene (**1**) to 3-methylene-1,5-hexadiene (**2**) suggest that this rearrangement occurs by two different pathways that diverge after passage through a common transition state.[4] A calculation in which geometries were optimized at the (8,8)CASSCF level with the 6-31G* basis set and energies at these geometries derived from single-point calculations using dynamic electron correlation at the (8,8)CASPT2/6-31G* level located allylic diradical intermediate **3** and two transition structures (TS_1 and TS_2) connecting it to **1** and **2**, respectively. When the geometries of intermediate points were constrained to prevent allylic conjugation, a pathway from TS_1 to TS_2 was found along which the energy decreased monotonically. The existence of a second pathway from **1** to **2**, that bypasses diradical **3**, is consistent with experimental results obtained by Roth and co-workers[5] which have shown that approximately half of this rearrangement proceeds without formation of a trappable intermediate. Furthermore, these results are consistent with the stereochemistry observed by Berson and Wessel[6] for the pyrolysis of (*R*,*E*)-5-methyl-1,2,6-octatriene (**4**), an optically active dimethyl derivative of **1**. They concluded that at least 16% of the rearrangement, which affords all four possible stereoisomers of 4-methyl-3-methylene-1,5-heptadiene (**5**), passes through cyclohexane-1,4-diyl diradicals (**6**).

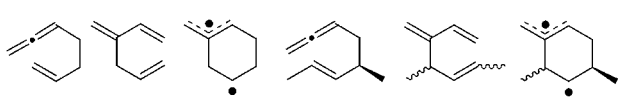

It has also been observed that the **1** → **2** rearrangement does not appear to benefit from allylic delocalization in its rate-determining transition structure (TS_1).[4] This led

† Lewis & Clark College undergraduate student.

(1) (a) Borden, W. T.; Loncharich, R. J.; Houk, K. N. *Annu. Rev. Phys. Chem.* **1988**, *39*, 213. (b) Houk, K. N.; Li, Y.; Evanseck, J. D. *Angew. Chem., Int. Ed. Engl.* **1992**, *31*, 682. (c) Houk, K. N.; Gonzalez, J.; Li, Y. *Acc. Chem. Res.* **1995**, *28*, 81. (d) Osamura, Y.; Kato, S.; Morokuma, K.; Feller, D.; Davidson, E. R.; Borden, W. T. *J. Am. Chem. Soc.* **1984**, *106*, 3362. (e) Morokuma, K.; Borden, W. T.; Hrovat, D. A. *J. Am. Chem. Soc.* **1988**, *110*, 4474. (f) Dupuis, M.; Murray, C.; Davidson, E. R. *J. Am. Chem. Soc.* **1991**, *113*, 9756. (g) Hrovat, D. A.; Morokuma, K.; Borden, W. T. *J. Am. Chem. Soc.* **1994**, *116*, 1072. (h) Kozlowski, P. M.; Dupuis, M.; Davidson, E. R. *J. Am. Chem. Soc.* **1995**, *117*, 774.

(2) Andersson, K.; Malmqvist, P.-Å.; Roos, B. O. *J. Chem. Phys.* **1992**, *96*, 1218.

(3) Kozlowski, P. M.; Davidson, E. R. *J. Chem. Phys.* **1994**, *100*, 3672.

(4) Hrovat, D. A.; Duncan, J. A.; Borden, W. T. *J. Am. Chem. Soc.* **1999**, *121*, 169.

(5) Roth, W. R.; Wollweber, D.; Offerhaus, R.; Rekowski, V.; Lennartz, H.-W.; Sustmann, R.; Müller, W. *Chem. Ber.* **1993**, *126*, 2701.

(6) Wessel, T. E.; Berson, J. A. *J. Am. Chem. Soc.* **1994**, *116*, 495.

10.1021/jo000571+ CCC: $19.00
Published on Web 09/01/2000

to the conclusion that the acceleration in rate observed experimentally for the allenyl Cope rearrangement of **1**, relative to the Cope rearrangement of 1,5-hexadiene, has its origin in the fact that the forming σ bond is stronger in the former (between an sp and sp^2 carbon) than in the latter (between two sp^2 carbons).

We have also recently reported on a theoretical study of the *conformationally restricted* allenyl Cope rearrangement of *syn*-7-allenylnorbornene (**7**) to racemic-**8**.[7] This rearrangement was found to involve two separate transition structures **9** and **10**, the latter 2.1 kcal/mol higher in enthalpy than the other, that both lead to common diradical intermediate **11**. In addition, a lower energy transition structure (**12**) was located between **11** and product **8**. The terminal methylene group of **7** was also shown to rotate in only one direction when passing through transition structure **9**, but to rotate freely in either direction when passing through transition structure **10**. This finding was shown to be remarkably consistent with the 90% stereoselectivity observed in the thermal Cope rearrangement of the dimethyl allenylnorbornene derivatives racemic-**13a** and racemic-**13b**.[8] Unlike the **1** → **2** allenyl Cope rearrangement, the **7** → **8** allenyl Cope rearrangement does appear to benefit from a measure of allylic resonance stabilization when passing through lower transition structure **9**, though not when passing through the slightly higher energy transition structure **10**.[7]

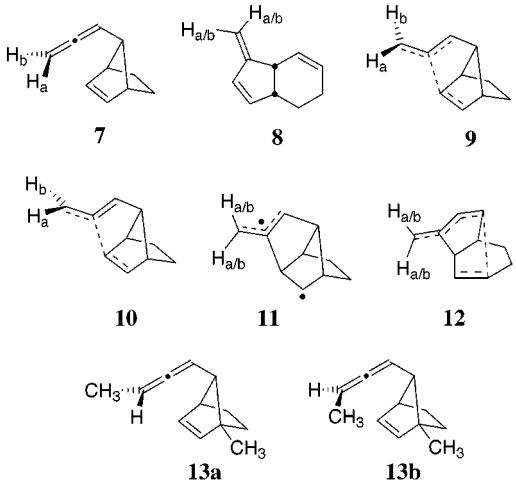

In the present theoretical study we examine several additional conformationally restricted Cope rearrangements. Results obtained on the allenyl Cope rearrangements of *syn*-5-propadienylbicyclo[2.1.0]pent-2-ene (**14**) and *syn*-6-propadienylbicyclo[2.1.1]hex-2-ene (**15**), in which respective tricyclic diradical intermediates **16** and **17** would be more highly strained than diradical **11**, are compared with those discussed above for the allenyl Cope rearrangements of **1** and **7**. In addition, we report on computational results obtained for the Cope rearrangements of *syn*-5-ethenylbicyclo[2.1.0]pent-2-ene (**18**), *syn*-6-ethenylbicyclo[2.1.1]hex-2-ene (**19**), and *syn*-7-vinylnorbornene (**20**). The results obtained on these vinyl systems are compared to those obtained on the corresponding allenyl Cope rearrangements of **14**, **15**, and **7**.

To our knowledge, there have been no reports of either experimental or theoretical studies of these Cope rearrangements in the literature. Preparations of **14**, **15**, **18**−**20**, and rearrangement products **22** and **24** (cf. Figure 1) have also not been reported in the literature,[9] however, preparations of rearrangement products **28**,[10] **32**,[11] and **38**[12] (cf. Figures 3, 4, and 6, respectively) have been reported.

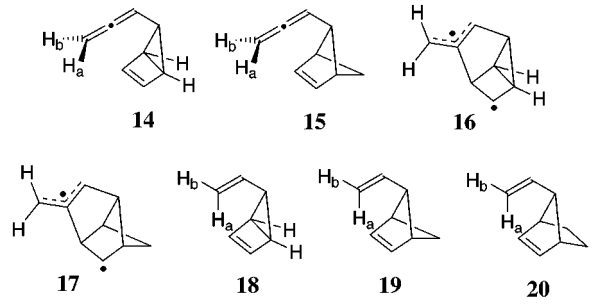

Computational Methodology

CASSCF calculations on all stationary points for the rearrangement of allenyl systems **14** and **15** (cf. Figure 1) were performed using an active space consisting of eight electrons in eight orbitals (i.e., the four σ and π bonding orbitals and their antibonding counterparts). Likewise, for all the stationary points obtained for the rearrangement of vinyl systems **18**−**20** (cf. Figures 3, 4, and 6), CASSCF calculations were performed using an active space of six electrons in six orbitals (i.e., the three σ and π bonding orbitals and their antibonding counterparts). Appropriate (8,8)CASSCF or (6,6)CASSCF vibrational analyses were carried out, through numerical frequency calculations, to characterize stationary points as energy minima (**14**, **15**, **18**−**20**, **22**, **24**, **26**, **28**, **30**, **32**, **36**, and **38**) or transition structures (**21**, **23**, **25**, **27**, **29**, **31**, **35**, and **37**) and to obtain zero-point energy differences. All CASSCF calculations made use of the Gaussian 94 suite of programs.[13]

The effects of dynamic electron correlation were included by performing the appropriate single-point (8,8)CASPT2 or (6,6)CASPT2 calculations at all stationary points using MOLCAS 4.[14] The 6-31G* basis set was used for both the CASSCF and CASPT2 calculations. These computational methods, taken together, have been shown to reproduce well the experimental enthalpies for the **1** → **2** allenyl Cope rearrangement.[4]

Three-dimensional structural representations of optimized geometries for structures **14**, **15**, **18**−**32**, and **35**−**38** prepared using MacMolPlt,[15] are shown in Figures 1, 3, 4, and 6.

(7) Duncan, J. A.; Azar, J. K.; Beathe, J. C.; Kennedy, S. R.; Wulf, C. M. *J. Am. Chem. Soc.* **1999**, *121*, 12029.

(8) (a) Duncan, J. A.; Hendricks, R. T.; Kwong, K. S. *J. Am. Chem. Soc.* **1990**, *112*, 8433. (b) Duncan, J. A. *J. Org. Chem.* **1996**, *61*, 4455.

(9) Although compound **18** has not been reported in the literature, its methyl derivative, *syn*-5-ethenyl-*anti*-5-methylbicyclo[2.1.0]pent-2-ene, has been reported as a transitory intermediate formed in the photolysis of 5-methyl-5-vinyl-1,3-cyclopentadiene: Burger, U.; Pamingle-Cristoforetti, E.; Bringhen, A. O. *Helv. Chim. Acta* **1988**, *71*, 389.

(10) Baldwin, J. E.; Belfield, K. D. *J. Org. Chem.* **1987**, *52*, 4772 and references therein.

(11) Roth, W. R.; Peltzer, B. *Ann. Chem.* **1965**, *685*, 56.

(12) Japenga, J.; Kool, M.; Klumpp, G. W. *Tetrahedron Lett.* **1974**, 3805.

(13) Frisch, M. J.; Trucks, G. W.; Schlegel, H. B.; Gill, P. M. W.; Johnson, B. G.; Robb, M. A.; Cheeseman, J. R.; Keith, T.; Petersson, G. A.; Montgomery, J. A.; Raghavachari, K.; Al-Laham, M. A.; Zakrzewski, V. G.; Ortiz, J. V.; Foresman, J. B.; Cioslowski, J.; Stefanov, B. B.; Nanayakkara, A.; Challacombe, M.; Peng, C. Y.; Ayala, P. Y.; Chen, W.; Wong, M. W.; Andres, J. L.; Replogle, E. S.; Gomperts, R.; Martin, R. L.; Fox, D. J.; Binkley, J. S.; Defrees, D. J.; Baker, J.; Stewart, J. P.; Head-Gordon, M.; Gonzalez, C.; Pople, J. A. Gaussian 94, Revision D.4; Gaussian, Inc.: Pittsburgh, PA, 1995.

(14) Andersson, K.; Blomberg, M. R. A.; Fülscher, M. P.; Karlström, G.; Lindh, R.; Malmqvist, P.-Å.; Neogrády, P.; Olsen, J.; Roos, B. O.; Sadlej, A. J.; Schütz, M.; Seijo, L.; Serrano-Andrés, L.; Siegbahn, P. E. M.; Widmark, P.-O. *MOLCAS*, version 4; University of Lund: Lund, Sweden, 1997.

(15) Bode, B. M.; Gorgon, M. S. *J. Mol. Graphics Mod.* **1998**, *16*, 133.

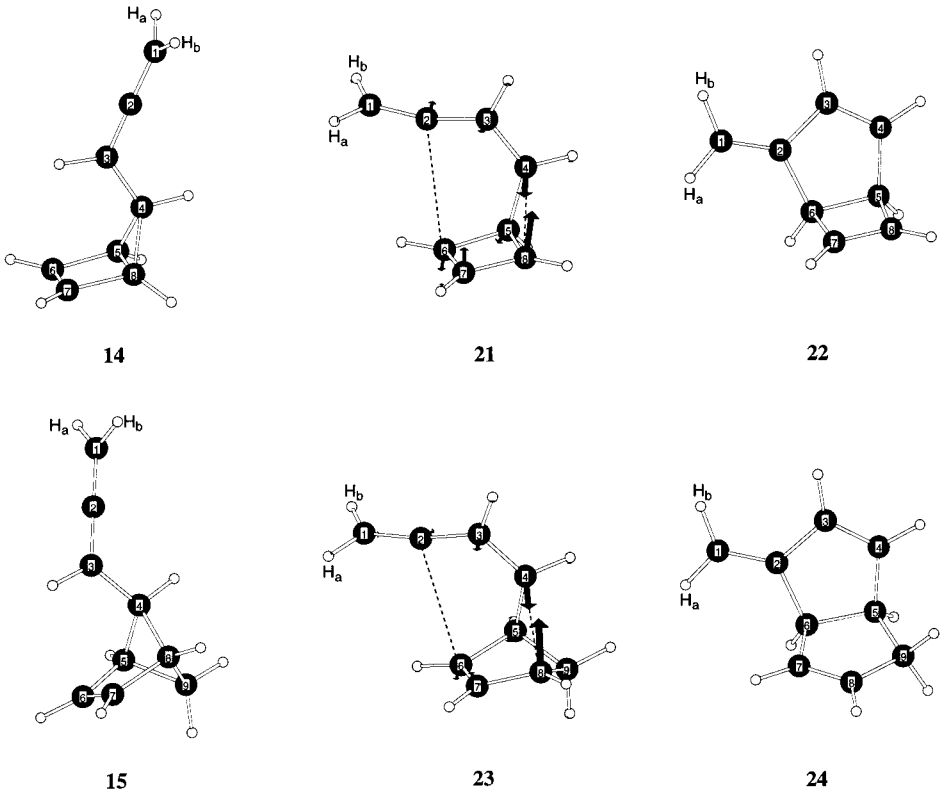

Figure 1. (8,8)CASSCF/6-31G*-optimized geometries for **14**, **15**, and **21**−**24**. Transition vectors are shown for transition structures **21** and **23**. Structures **14**, **15**, **22**, and **24** were frequency characterized as minima and imaginary frequencies for transition structures **21** and **23** were found to be −278 and −346 cm^{-1}, respectively. $H_bC_1C_3H$ dihedral angles in **21** and **23** are 81.8° and 85.3°, respectively.

Table 1. Carbon−Carbon Distances (Å) for the Stationary Points on the (8,8)CASSCF Potential Surface for the Cope Rearrangements of *syn*-5-Propadienylbicyclo[2.1.0]pent-2-ene (14) to Triene 22 and *syn*-6-Propadienylbicyclo[2.1.1]hex-2-ene (15) to Triene 24. Obtained with the 6-31G* Basis Set

structure	C_1-C_2	C_2-C_3	C_3-C_4	C_4-C_5	C_5-C_6	C_6-C_7	C_7-C_8	C_5-C_8	C_8-C_9	C_5-C_9	C_4-C_8	C_2-C_6
14	1.32	1.32	1.49	1.51	1.52	1.35	1.52	1.51			1.55	
15	1.32	1.32	1.50	1.56	1.53	1.34	1.53		1.55	1.55	1.61	
21	1.32	1.35	1.42	1.49	1.53	1.38	1.43	1.51			2.24	2.94
22	1.34	1.47	1.35	1.51	1.57	1.52	1.34	1.53				1.55
23	1.32	1.34	1.44	1.53	1.53	1.36	1.46		1.52	1.53	2.42	3.00
24	1.34	1.47	1.34	1.51	1.56	1.51	1.34		1.51	1.55		1.56

Molecular orbitals were visualized using Spartan.[16] Transition vectors, obtained from the appropriate CASSCF/6-31G* numerical frequency analyses, are also shown for transition structures **21**, **23**, **25**, **27**, **29**, **31**, **35**, and **37**. Calculated carbon−carbon bond lengths for the structures in Figure 1 (**14**, **15**, and **21**−**24**) are assembled in Table 1, for the structures in Figures 3 and 4 (**18**, **19**, and **25**−**32**) in Table 2 and for the structures in Figure 6 (**20** and **35**−**38**) in Table 3. CASSCF/6-31G*-optimized geometries and both CASPT2/6-31G* and CASSCF/6-31G* energies for all structures in Tables 1−3 are included in the Supporting Information.

Results and Discussion

Calculations on the 14 → 22 and 15 → 24 Allenyl Cope Rearrangements (cf. Figures 1 and 2 and Table 1). *syn*-5-Propadienylbicyclo[2.1.0]pent-2-ene (**14**) and its Cope rearrangement product **22** were successfully optimized at the (8,8)CASSCF/6-31G* level with the correct active space orbitals in each case. Not surprisingly, we were unsuccessful in optimizing a potential diradical intermediate, corresponding to drawing **16**, which would be expected to be highly strained. Interestingly, we located only a single transition structure **21** on the potential energy surface (PES), for a concerted reaction between **14** and **22**. This was confirmed by the motion of the transition vector (cf. Figure 1) and intrinsic reaction coordinate (IRC) calculations.[17] The computed energy differences between the zero-point corrected enthalpies of **14**, **21**, and **22** at both the (8,8)CASSCF/6-31G*//(8,8)CASSCF/6-31G* and (8,8)CASPT2/6-31G*//(8,8)CASSCF/6-31G* levels of theory are shown in Figure 2a.

(16) *SPARTAN*, Version 5.0, Wavefunction, Inc. 18401 Von Karman Avenue, Suite 370, Irvine, CA 92715.

(17) In all cases, the geometries of the final structures that could be obtained on either side of all transition structures (i.e., **21**, **23**, **25**, **27**, **29**, **31**, **35**, and **37**) by the IRC method closely resembled the minimum structures shown in Figures 1, 3, 4, and 6. Furthermore, in many cases these final IRC structures were readily optimized to their corresponding minimum structures with the exact geometries depicted in these figures. In particular, fully optimized Cope products **22**, **24**, **28**, **32**, and **38** were obtained in this way, as were diradicals **26** from both **25** and **27**, **30** from **31**, and **36** from both **35** and **37**. Also, optimization of the final IRC structure leading to reactant **15** led to a conformation of **15** with a HC_3C_4H dihedral angle of −61.8°. Similarly, optimizations of the final IRC structures leading to reactants **18** and **19** led to conformations of **18** and **19** with HC_2C_3H dihedral angles of −41.7° and −65.6°, respectively.

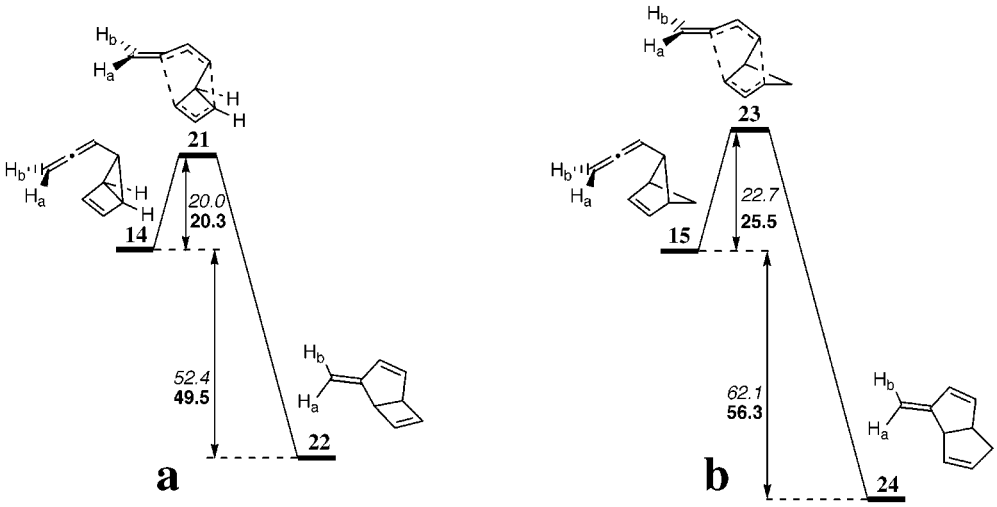

Figure 2. Reaction coordinate diagram showing zero-point corrected enthalpy differences (in kcal/mol) among structures optimized at the (8,8)CASSCF/6-31G* level; (8,8)CASSCF/6-31G* energies are shown in italics and (8,8)CASPT2/6-31G* energies in boldface type: (a) concerted **14** → **22** rearrangement; (b) concerted **15** → **24** rearrangement.

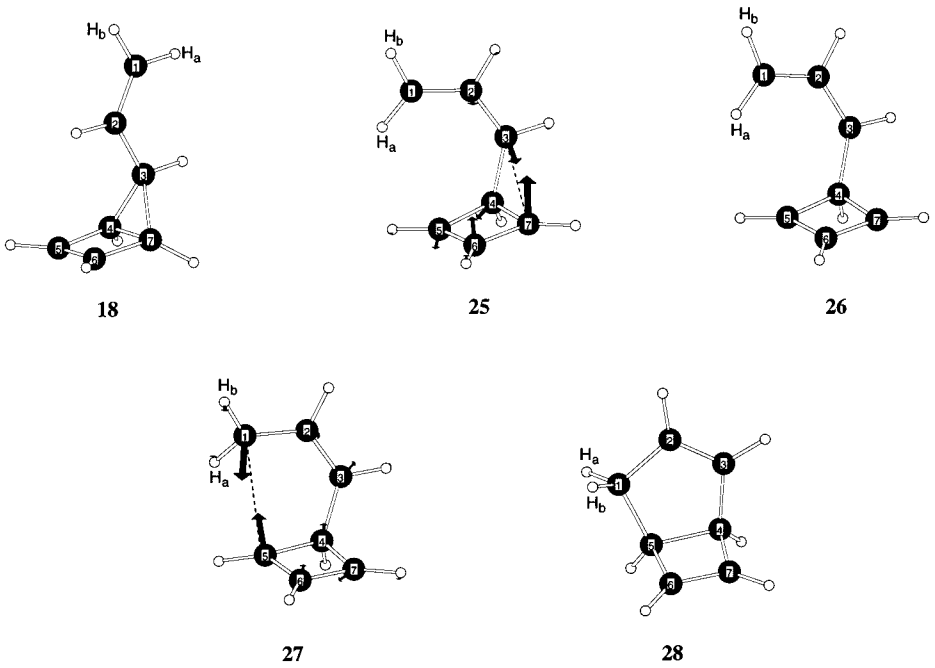

Figure 3. (6,6)CASSCF/6-31G*-optimized geometries for **18** and **25**−**28**. Transition vectors are shown for transition structures **25** and **27**. Structures **18**, **26**, and **28** were frequency characterized as minima and imaginary frequencies for transition structures **25** and **27** were found to be −263 and −383 cm^{-1}, respectively. HC_2C_3H and HC_3C_4H dihedral angles in diradical **26** are −5.4° and −49.4°, respectively.

Similarly, *syn*-6-propadienylbicyclo[2.1.1]hex-2-ene (**15**) and its allenyl Cope rearrangement product **24** were optimized at the same level of theory. We were able to optimize the corresponding tricyclic diradical intermediate (**17**) in this case.[18] However, no transition structures linking **17** to **14** or **24** could be located. Instead, we again found a single transition structure (**23**), characteristic of a **15** → **24** concerted rearrangement. This was once again confirmed by the motion of the transition vector for **23** (cf. Figure 1) as well as by IRC calculations.[17] The computed energy differences between the zero-point corrected enthalpies of **15**, **23**, and **24** are shown in Figure 2b.

As shown in Figures 1 and 2, computational results obtained for the **14** → **22** and **15** → **24** allenyl Cope rearrangements are similar in many respects. Transition structures **21** and **23** have similar geometries and, in accordance with the Hammond Postulate,[19] they both occur early along the reaction coordinate with C_2-C_6 distances of 2.94 and 3.00 Å, respectively (cf. Table 1). Transition structures **21** and **23** have been fully characterized as first-order saddle points on their respective PE surfaces, despite long C_2-C_6 and C_4-C_8 distances (the latter 2.24 and 2.42 Å, respectively) that make them resemble weakly interacting diallylic diradicals (cf. Figure 1 and Table 1). Both reactions are also found to be "stereospecific" in the same sense, that is the terminal methylene group is observed to rotate only as shown in

(18) At the (8,8)CASSCF/6-31G*//(8,8)CASSCF/6-31G* level, optimized diradical **17** is only 0.3 kcal/mol below that for concerted transition structure **23**. At the (8,8)CASPT2/6-31G*//(8,8)CASSCF/6-31G* level, however, it is 13.4 kcal/mol lower.

(19) Hammond, G. S. *J. A. Chem. Soc.* **1955**, *77*, 334.

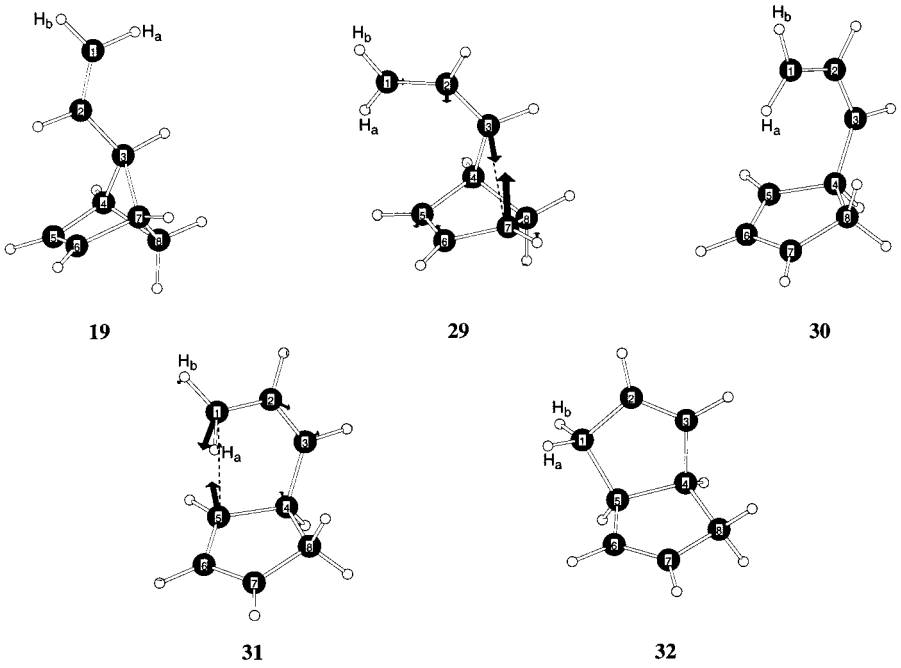

Figure 4. (6,6)CASSCF/6-31G*-optimized geometries for **19** and **29**−**32**. Transition vectors are shown for transition structures **29** and **31**. Structures **19**, **30**, and **32** were frequency characterized as minima and imaginary frequencies for transition structure **29** and **31** were found to be −357 and −433 cm^{-1}, respectively. HC_2C_3H and HC_3C_4H dihedral angles in diradical **30** are −0.4° and −4.7°, respectively.

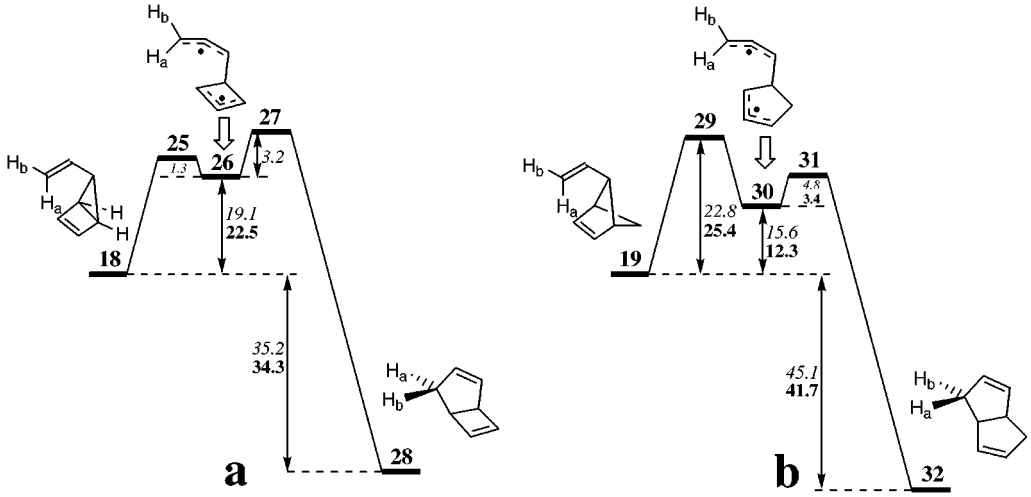

Figure 5. Reaction coordinate diagram showing zero-point corrected enthalpy differences (in kcal/mol) among structures optimized at the (8,8)CASSCF/6-31G* level; (8,8)CASSCF/6-31G* energies are shown in italics and (8,8)CASPT2/6-31G* energies in boldface type: (a) nonconcerted **18** → **28** rearrangement; (b) nonconcerted **19** → **32** rearrangement.

Table 2. Carbon−Carbon Distances (Å) for the Stationary Points on the (6,6)CASSCF Potential Surface for the Cope Rearrangements of *syn*-5-Ethenylbicyclo[2.1.0]pent-2-ene (18) to Diene 28 and *syn*-6-Ethenylbicyclo[2.1.1]hex-2-ene (19) to Diene 32. Obtained with the 6-31G* Basis Set

structure	C_1-C_2	C_2-C_3	C_3-C_4	C_4-C_5	C_5-C_6	C_6-C_7	C_4-C_7	C_7-C_8	C_4-C_8	C_3-C_7	C_1-C_5
18	1.34	1.49	1.51	1.52	1.35	1.52	1.51			1.55	
19	1.34	1.50	1.56	1.53	1.34	1.53		1.55	1.55	1.61	
25	1.36	1.42	1.49	1.53	1.37	1.43	1.51			2.24	3.12
26	1.38	1.40	1.50	1.53	1.39	1.40	1.53			2.49	3.18
27	1.42	1.37	1.50	1.54	1.41	1.38	1.53			2.46	2.71
28	1.51	1.34	1.51	1.57	1.52	1.34	1.52				1.57
29	1.36	1.44	1.53	1.53	1.36	1.46		1.52	1.53	2.41	3.13
30	1.39	1.40	1.51	1.52	1.39	1.39		1.51	1.56	3.69	3.36
31	1.44	1.36	1.51	1.52	1.41	1.37		1.51	1.56	3.67	2.75
32	1.51	1.34	1.51	1.56	1.51	1.34		1.51	1.55	3.32	1.58

Figure 2a,b. This is the direction of rotation predicted by the Woodward−Hoffmann rules for concerted pericyclic reactions.[20] However, this direction of rotation also appears to result in less framework distortion for both the **14** → **22** and **15** → **24** rearrangements. Finally, as shown in Figure 2, the activation enthalpies are comparable, with the **15** → **24** rearrangement being 4.2 kcal/mol (i.e., 16%) higher at the CASPT2/6-31G* level. This

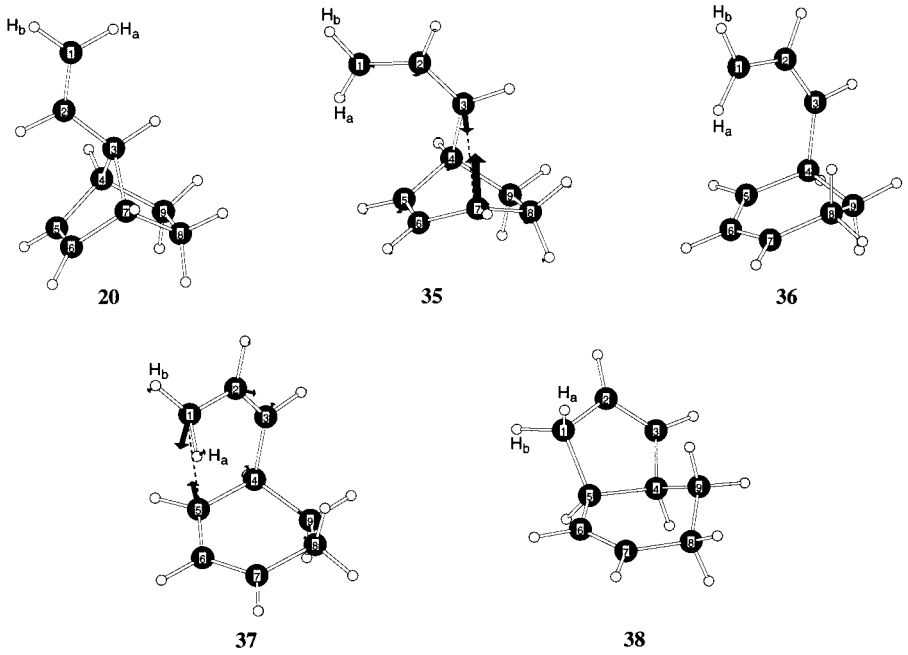

Figure 6. (6,6)CASSCF/6-31G*-optimized geometries for **20** and **35**−**38**. Transition vectors are shown for transition structures **35** and **37**. Structures **20**, **36**, and **38** were frequency characterized as minima and imaginary frequencies for transition structures **35** and **37** were found to be −299 and −419 cm^{-1}, respectively. HC_2C_3H and HC_3C_4H dihedral angles in diradical **36** are 1.8° and −34.7°, respectively.

Table 3. Carbon−Carbon Distances (Å) for the Stationary Points on the (6,6)CASSCF Potential Surface for the Cope Rearrangement of *syn*-7-Vinylnorbornene (20) to Diene 38. Obtained with the 6-31G* Basis Set

structure	C_1-C_2	C_2-C_3	C_3-C_4	C_4-C_5	C_5-C_6	C_6-C_7	C_7-C_8	C_8-C_9	C_4-C_9	C_3-C_7	C_1-C_5
20	1.34	1.50	1.55	1.52	1.34	1.52	1.55	1.56	1.55	1.58	
35	1.37	1.42	1.52	1.52	1.35	1.45	1.51	1.54	1.54	2.71	3.17
36	1.39	1.40	1.52	1.51	1.39	1.39	1.51	1.53	1.55	3.90	3.25
37	1.45	1.35	1.52	1.52	1.41	1.38	1.51	1.53	1.54	3.85	2.80
38	1.51	1.34	1.51	1.55	1.51	1.34	1.51	1.53	1.54		1.58

small difference may reflect a greater release of strain for ring opening in **14** relative to **15**.

In the nonconcerted **7** → **8** rearrangement, that proceeds through diradical intermediate **11**, we demonstrated that the terminal allenyl π-bond plays a direct role in the formation of rate-determining transition structures **9** and **10**, especially in the latter where the terminal carbon−carbon bond distance increases from 1.32 Å in **7** to 1.41 Å in **10**.[7] As the C_1-C_2 bond distance in both transition structures **21** and **23** is 1.32 Å (cf. Figure 1 and Table 1), the same as in **14** and **15**, the allenyl π-bond plays no such direct role in the **14** → **22** and **15** → **24** rearrangements. Finally, the (8,8)CASPT2/6-31G*//(8,8)CASSCF/6-31G* activation enthalpies for these rearrangements (20.3 and 25.5 kcal/mol, respectively) are lower than the lower of the two values calculated for the **7** → **8** rearrangement (30.6 kcal/mol),[7] presumably because of the partial release of ring strain in ascending from either **14** or **15** to their respective transition structures on the PES.

Calculations on the 18 → 28 and 19 → 32 Cope Rearrangements (cf. Figures 3−5 and Table 2). To further define the role played by the allenyl group, relative to a vinyl group, in these Cope rearrangements, we also studied the **18** → **28** and **19** → **32** rearrangements computationally. More specifically, we were interested in determining if these rearrangements would also be concerted at the same level of computational theory used to study the **14** → **22** and **15** → **24** rearrangements. Interestingly, as summarized in Figure 5, parts a and b, both rearrangements were shown to be nonconcerted on the (6,6)CASSCF/6-31G* PES and to involve diallylic monocyclic diradicals **26** and **30**, respectively, formed through cleavage of the respective C_3-C_7 bridgehead bonds. The connectivity, shown in Figure 5a,b, was again fully demonstrated by the motion of the transition vectors in structures **25**, **27**, **29**, and **31** (cf. Figures 3 and 4) and by IRC calculations.[17] Also, no evidence was found for any pathway involving highly strained and nonallylic tricyclic cyclohexane-1,4-diyl intermediates, comparable to **16** and **17** (in the allenyl case), that might derive from initial C_1-C_5 bond formation. Thus, in the rearrangements of **18** and **19**, the resonance stabilization provided by the two allylic radicals present in both **26** and **30** apparently outweigh any advantage of the initial formation of a new σ bond, either to form cyclohexane-1,4-diyl intermediates or, alternatively, products **28** and **32** directly via concerted pathways.

As shown in Figure 5a, the **18** → **28** rearrangement shows a very shallow minimum for diradical **26** on the (6,6)CASSCF/6-31G* PES. The rate-determining transition structure **27**, between diradical **26** and product **28**,

(20) (a) The concerted **14** → **22** and **15** → **24** rearrangements may be viewed in the Woodward−Hoffmann formalism[20b] as $\sigma 2s + \pi 2s + \pi 2s$ processes, i.e., ones in which each of the three 2-electron components is employed in a suprafacial manner. Such a $\sigma 2s + \pi 2s + \pi 2s$ process dictates that the terminal methylene group of **14** and **15** should rotate only in the direction shown in Figure 2a,b.[8a] (b) Woodward, R. B.; Hoffmann, R. *The Conservation of Orbital Symmetry*; Verlag Chemie: Weinheim, Germany, and Academic Press: New York, 1970.

is found to be 3.2 kcal/mol in enthalpy above **26**, and transition structure **25** only 1.3 kcal/mol above. Moreover, when (6,6)CASPT2/6-31G* energy "corrections" were applied to the zero-point corrected (6,6)CASSCF/6-31G* enthalpies of **25**−**27**, **26** was found, awkwardly enough, to have the highest energy (1.4 kcal/mol higher than **25** and 0.2 kcal/mol higher than **27**).

As shown in Figure 5b, the corresponding (6,6)CASSCF/6-31G* PES for the **19** → **32** rearrangement shows a much deeper minimum for the comparable diradical intermediate (**30**). The enthalpy difference between rate-determining transition structure **29** and diradical **30**, calculated at the (6,6)CASPT2/6-31G*//(6,6)CASSCF/6-31G* level, was observed to be 13.1 kcal/mol and between transition structure **31** and diradical **30**, 3.4 kcal/mol. As shown in Figure 5, the overall activation enthalpies for the **18** → **28** and **19** → **32** rearrangements are similar. The most striking difference between the (6,6)CASSCF/6-31G* PE surfaces for the rearrangements of **18** and **19** relate to the opposite direction of rotation of the terminal methylene groups, as also shown in Figure 5. The direction of rotation observed in the **18** → **28** case can be characterized as Woodward−Hoffmann allowed,[20b] and that for **19** → **32** as Woodward−Hoffmann forbidden.[20b] Since the computational results suggest these reactions are nonconcerted, however, the Woodward−Hoffmann rule would not be expected to apply. The observed "stereospecificity" appears to relate to the different conformations favored for the minimum diradical structures **26** and **30**.[21] In the case of diradical **26**, the p-orbital lobe on C_1 that would extend in an outward direction from the page in Figure 3, may more readily overlap with the accessible p-orbital lobe on C_5 to form product **28** through transition structure **27**. In the case of diradical **30**, however, it is the oppositely directed p-orbital lobe on C_1 (i.e., extended in a mostly inward direction to the page in Figure 4) that may more readily overlap with the p-orbital on C_5 to form product **32** through transition structure **31**. This difference may perhaps best be viewed by comparing the conformations of optimized transition structures **27** and **31** as depicted in Figures 3 and 4, respectively.

Since the **18** → **28** and **19** → **32** rearrangements are shown by our calculational method to involve diallylic diradical intermediates **26** and **30**, respectively, we decided to search for comparable intermediates in the allenyl cases; diradicals **33** and **34** might be involved in nonconcerted alternative pathways for the **14** → **22** and **15** → **24** rearrangements discussed above. A diradical corresponding to drawing **33** could not be located on the (8,8)CASSCF/6-31G* PES. Although one corresponding to drawing **34**, with a (8,8)CASPT2/6-31G*//(8,8)CASSCF/6-31G* enthalpy 14.6 kcal/mol higher that **15**, was located (optimized coordinates included with Supporting Information), no transition structure connecting it to either **15** or **24** could be found. Furthermore, when transition structure **29**, in the corresponding vinyl case, was altered[22] by the addition of a carbon−carbon double bond to the end of the free vinyl group and optimized, the structure that resulted was equivalent in all respects to

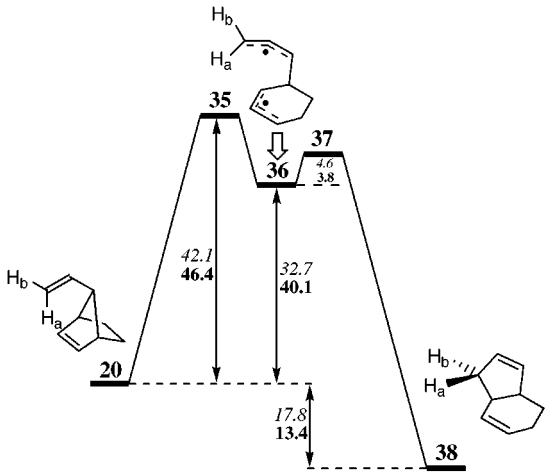

Figure 7. Reaction coordinate diagram showing zero-point corrected enthalpy differences (in kcal/mol) among structures **20** and **35**−**38**, optimized at the (8,8)CASSCF/6-31G* level; (8,8)CASSCF/6-31G* energies are shown in italics and (8,8)-CASPT2/6-31G* energies in boldface type.

concerted transition structure **23**. (Comparable alteration of transition structure **31** resulted in convergence failure upon attempted optimization. Convergence failures were also the result of attempted optimizations of similarly altered transition structures **25** and **27**.) Thus, it appears likely that the concerted pathways described in the previous section for the **14** → **22** and **15** → **24** rearrangements are the only existing ones.

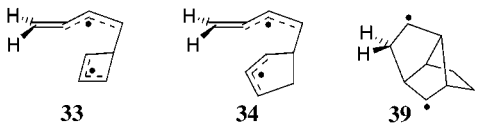

Calculations on the 20 → 38 Cope Rearrangement (cf. Figures 6 and 7 and Table 3). Since in a previous paper[7] we described the allenyl Cope rearrangement of allenylnorbornene **7**, we decided, for completeness, to map the PES for the Cope rearrangement of its corresponding vinyl system. We found the rearrangement of *syn*-7-vinylnorbornene (**20**) to diene **38** to most closely parallel the rearrangement of **19**. As shown in Figure 7, the **20** → **38** rearrangement proceeded, like the **19** → **32** one, with rotation of the terminal methylene group in a direction formally opposite to that predicted by the Woodward−Hoffmann rules for concerted pericyclic reactions.[20b] The reason for this "stereospecificity" is probably the same as that proposed above for the "stereospecificity" observed in the **19** → **32** case. The connectivity, shown in Figure 7, was once again demonstrated by the motion of the transition vectors in structures **35** and **37** and by IRC calculations.[17] Although we were able to optimize a tricyclic cyclohexane-1,4-diyl corresponding to drawing **39**, we found no evidence that it was connected to **20** or **38** on a PES. The CASPT2/6-31G* enthalpy difference between diradical **36** and product **38** is 53.5 kcal/mol (cf. Figure 7). This closely parallels the energy differences between diradical **26** and product **28** (56.8 kcal/mol) and between diradical **30** and product **32** (54.0 kcal/mol) for

(21) The geometry of diradical intermediates **26** and **30** depicted in Figures 3 and 4 respectively, represent the most stable optimized structures with HC_2C_3H dihedral angles close to 0° and HC_3C_4H dihedral angles less than 90°, i.e., conformations best suited to form transition structures **25** and **27** in the case of diradical **26** and transition structures **29** and **31** in the case of diradical **30**. Of course, corresponding diradicals with HC_3C_4H and HC_2C_3H dihedral angles ≈180° are more stable.

(22) The additional carbon−carbon double bond was added to optimized structure **27** in the Spartan[12] model builder. The terminal allenyl methylene group of the resulting starting structure was oriented such that it was approximately perpendicular to the terminal vinyl methylene group it replaced.

the Cope rearrangements of **18** and **19**, respectively (cf. Figure 5). The major difference between the Cope rearrangement of **20** on one hand and those of **18** and **19** on the other is the far larger activation energy calculated for the **20** → **38** rearrangement. This difference presumably reflects the greater stability of the bicyclic ring in **20** versus those in **18** and **19**.

Comparison of the Cope Rearrangements of the Allenyl (14, 15, and 7) and Corresponding Vinyl (18, 19, and 20) Systems. By comparing Figures 2b and 5b, it can be seen that the Cope rearrangements of **15** and **19** are predicted to have nearly identical CASPT2/6-31G*//CASSCF/6-31G* (and CASSCF/6-31G*//CASSCF/6-31G*) activation enthalpies. Although a full comparison of CASPT2/6-31G*//CASSCF/6-31G* energies is not possible for the corresponding Cope rearrangements of **14** and **18** shown in Figures 2a and 5a, it can be seen that diradical intermediate **26** is 22.5 kcal/mol above **18**, while transition structure **21** is only 20.3 kcal/mol above **14**. Thus the Cope rearrangement of **14** appears to be at least slightly favored over **18**. As shown in Figure 7, the (6,6)-CASPT2/6-31G*//(6,6)CASSCF/6-31G* activation enthalpy for the Cope rearrangement of vinylnorbornene **20** is 46.4 kcal/mol. This is significantly higher than the 30.6 kcal/mol enthalpy difference between **7** and **9** and the 32.7 kcal/mol difference between **7** and **10**, calculated for the two pathways involved in the rearrangement of **7**. The more favorable activation enthalpy for the **7** → **8** allenyl Cope rearrangement can at least partially be ascribed to the direct participation of the terminal allenyl π-bond in the rearrangement process, a process we have termed an "augmented" Cope rearrangement.[7] If the **14** → **22** and **15** → **24** rearrangements were augmented in a similar way, this might explain why the pathways are concerted as opposed to the **18** → **28** and **19** → **32** ones which appear to proceed by way of diradicals **26** and **30**, respectively. However, as discussed above, our computational results make it clear that the **14** → **22** and **15** → **24** rearrangements are not augmented as is the **7** → **8** rearrangement. What is it then that causes the allenyl **14** → **22** and **15** → **24** Cope rearrangements (cf. Figure 2) to be concerted while their **18** → **28** and **19** → **32** vinyl counterparts (cf. Figure 5) are nonconcerted? Even though the forming σ bonds in transition structures **21** and **23** (cf. Figure 2 and Table 1) are relatively long and weak, it may be that because these bonds are between sp and sp^2 carbons (C_2 and C_6) in transition structures **21** and **23**, the balance is tipped in favor of concertedness for the **14** → **22** and **15** → **24** rearrangements. By contrast, the corresponding **18** → **28** and **19** → **32** rearrangements can only form weaker σ bonds between two sp^2 carbons (C_1 and C_5 in Figures 3 and 4). In this one particular way, at least, the conformationally restricted allenyl Cope rearrangements of **14** and **15** resemble the rearrangement of conformationally flexible **1**[4] more than the conformationally restricted rearrangement of **7**.[7] However, as the allenyl Cope rearrangements of **1** and **7** both involve diradical intermediates, the *concerted* allenyl Cope rearrangements of **14** and **15** are currently in a class by themselves.

Conclusions

We have performed calculations on the conformationally restricted allenyl Cope rearrangements of **14** and **15** which finds them to be concerted at the (8,8)CASSCF/6-31G* level of theory. To our knowledge, these are the first examples of concerted *allenyl* Cope rearrangements to be reported. Insights into the reasons for concertedness in these systems are drawn from comparisons with other allenyl Cope rearrangements (**1** → **2** and **7** → **8**) and the conformationally restricted Cope rearrangements of corresponding vinyl systems **18**, **19**, and **20**, none of which have been found to be fully concerted. The allenyl Cope rearrangements of **14** and **15** may partially derive their concertedness from the relative instability of intermediate diradicals **16** and **17** when compared to diradicals **3** and **11**, involved in the rearrangements of **1** and **7**, respectively. However, diallylic diradicals **33** and **34** are also not involved in the **14** → **22** and **15** → **24** rearrangements, even though such diradicals (**26** and **30**) are involved in the corresponding Cope rearrangements of vinyl systems **18** and **19**. Thus a second contributing factor favoring concertedness in the **14** → **22** and **15** → **24** rearrangements may stem from the opportunity that exists for the formation of a stronger sp-sp^2 carbon−carbon σ bond in these rearrangements, relative to a weaker sp^2-sp^2 carbon−carbon σ bond in the corresponding **18** → **28** and **19** → **32** rearrangements.

Acknowledgment. Support for this work from the John S. Rogers Science Research Program of Lewis & Clark College is gratefully acknowledged. We are also grateful to the National Science Foundation (grant DUE−9750586) for providing funds for the purchase of several Silicon Graphics workstations used in the computations. We are especially indebted Mr. Brian Arthur, System Administrator at Lewis & Clark College, for his technical assistance. We also thank Professor Stephen Tufte, of the Lewis & Clark College Physics Department, for the use of his R12000 Silicon Graphics workstation.

Supporting Information Available: CASSCF/6-31G*-optimized geometries and CASPT2/6-31G* and CASSCF/6-31G* energies for structures **14**, **15**, **18**−**32**, and **34**−**38**. This material is available free of charge via the Internet at http://pubs.acs.org.

JO000571+